Desalination and Water Treatment
www.deswater.com
doi: 10.5004/dwt.2022.28743

269 (2022) 163–175
September

Production of microcapsule biosorbent of functionalized Lycopodium Clavatum Sporopollenin (Sp-CPTS-AHP) and its application to Cr(III) ions

Aysel Cimen[a,*], Ali Bilgiç[b], Savaş Polat[a]

[a]*Department of Chemistry, Kamil Ozdag Science Faculty, Karamanoglu Mehmetbey University, 70100 Karaman, Turkey, Phone: 90 0338 2262157; email: ayselcimen42@hotmail.com (A. Cimen), Phone: 90 0338 226257; email: ayselcimen42@hotmail.com (S. Polat)*
[b]*Vocational School of Technical Sciences, Karamanoglu Mehmetbey University, 70100 Karaman, Turkey, Phone: 90 0338 2262169; email: alibilgic100@hotmail.com*

Received 18 March 2022; Accepted 16 July 2022

ABSTRACT

3-(Chloropropyl)-trimethoxysilane (CPTS) was modified on Lycopodium Clavatum Sporopollenin microcapsules (Sp) with the aim of obtaining the Sp-CPTS compound. 2-amino-3-hydroxypyridine (AHP) was immobilized on Sp-CPTS and a microcapsule adsorbent surface (Sp-CPTS-AHP) was prepared. This surface was prepared to effectively remove Cr(III) in the solution. The surface of Sp-CPTS-AHP microcapsule biosorbent was successfully characterized by Fourier-transform infrared spectroscopy and scanning electron microscopy. Some experimental parameters (pH, contact time, amount of biosorbent, temperature and concentration) affecting the removal of Cr(III) were investigated. Adsorption isotherm models were utilized to explain the adsorption event on the microcapsule biosorbent. As a result of Cr(III) application with Sp-CPTS-AHP microcapsule biosorbent, approximately 70% Cr(III) removal was obtained at pH 6. The $\Delta H°$ value calculated for the Cr(III) in the solution at temperatures between 25°C–50°C is 29.31 kJ mol^{-1} and the $\Delta S°$ value is 235.88 J mol^{-1} K^{-1}. The mean adsorption energy for the Sp-CPTS-AHP microcapsule biosorbent was calculated as 0.893, 1.271, 1.549 and 2.744 kJ mol^{-1} for 298, 308, 319 and 328 K, in Cr(III) solution respectively. According to the parameters interpreted from the experimental data, the best Cr removal was attained at pH = 6.0, 0.03 g adsorbent, 298 K temperature, 30 mg L^{-1} initial concentration and 90 min contact time. The correlation coefficient (q_e) calculated with the pseudo-second-order model is 14.993 mg g^{-1} and the correlation coefficient calculated with the pseudo-first-order model is 7.568 mg g^{-1}. Langmuir maximum adsorption capacity (q_m) is 17.668, 19.646, 20.704 and 21.929 mg g^{-1} for 298°C, 308°C, 318°C and 328°C, respectively. The newly synthesized microcapsule adsorbent surface has shown significant success in removing Cr(III) from the solution. Therefore, it can be recommended for the effective removal of heavy metals from water.

Keywords: Sporopollenin; Microcapsule biosorbent; Cr(III); Adsorption; Isotherm

1. Introduction

The pollution of natural waters is dependent to the enlargement of cities and slums and to the development of industries and of agriculture, based on the use of various chemicals. This results into a number of toxic and harmful discharges, including heavy metals, nitrates, phosphates, and pesticides, into natural ecosystems and hydrosystems [1–3]. Pollution of the environment by toxic heavy metals is a especially common problem with pollution sources due mainly to industrial activities. These

* Corresponding author.

1944-3994/1944-3986 © 2022 Desalination Publications. All rights reserved.

heavy metals are unloading, directly or indirectly, into environmental waters, particularly in developing countries. In addition, many studies have shown the existence of traces of heavy metals in marine waters and ecosystems and their influence on the aquatic environments and animal health [4,5]. Heavy metal pollution is one of the most critical environmental problems [6]. Indeed, these metals are usually toxic, even at very low concentrations, and non-biodegradable and frequently resist to traditional removal treatments. Therefore, they can severely degrade the quality of drinking water resources.

As a result, it is very significant to improve effective methods of removing these pollutants from wastewater, before pouring into the natural water system, for maintain the concentration limits set by the international standards. These methods are membrane, photocatalyst, electrodialysis and adsorption etc. [7–9]. The adsorption method is preferred because it is cheap, easy to apply and has high separation properties.

Chrome, electrical plating, leather making, wood preservatives, paint manufacturing, printing and paper, plastic coatings and textile industries etc. used in industrial processes [10–13]. Great amounts of chromium-containing wastewater from different industries are discharged into the environment [7]. The dominant chromium species in wastewater are Cr(III) and Cr(VI) ions. Hexavalent chromium (Cr(VI)) is 500–1,000 times more toxic than trivalent chromium. This metal needs to be removed from wastewater due to its harmful effects on the body and its cumulative properties and its non-biodegradability. At the same time, trivalent chromium should be removed from wastewater because Cr(III) ions are easily converted to Cr(VI) in the environment [10].

If Cr(III) amount exceeds the exposure limit in the human body, it causes diseases such as depression, Alzheimer's, speech disorders, mood swings and allergic reaction [14–16]. Since WHO has determined the mean limit value of Cr(III) in drinking water to be 0.05 mg L^{-1} [17,18], maximum care should be taken not to exceed 0.05 mg L^{-1} of Cr(III) in drinking water [19].

Sp is a microcapsule biosorbent that is steady as molecular construction, durable to chemical materials, the ability of high adsorption, appropriate for the modification, effortless to acquire and cheap. In this study, the starting material of the prepared adsorbent is Sporopollenin and its surface was modified with 3-(chloropropyl)-trimethoxysilane (CPTS) compound. This surface was then immobilized with AHP.

The thermodynamics and kinetic features concerning the adsorption of Cr(III) on the Sp-CPTS-AHP have been researched [19]. Besides, the influence of experimental factors such as pH, touch duration, adsorbent quantity, temperature and different concentrations were researched to eliminate Cr(III) in solution. As the outcomes are much yielding and harmonious with the literature, Sp-CPTS-AHP adsorbent can be easily recommended for Cr(III) removal from aqueous solution [19].

Since the starting material of the adsorbent used in this study is a herbal microcapsule and it was prepared for the first time, it can be said that the study is original. The cheapness of the method used, the environmental friendliness of the material and the high percentage of removal of Cr(III) ions from wastewater increase the novelty and attractiveness of this study.

2. Experimental

2.1. Substances and devices

Microcapsules (particle size 20 μm) of Lycopodium Clavatum Sporopollenin, the starting material of the microcapsule biosorbent we prepared, were obtained from Fluka (Fluorochem Limited, London, United Kingdom). 3-(Chloropropyl)-trimethoxysilane ($C_6H_{15}ClO_3Si$ and ≥97%), toluene (Anhydrous, 99.8%), methanol (Anhydrous, 99.8%), sodium hydroxide, nitric acid (99.8%), ethanol liquid (clear, colorless), diethyl ether (Anhydrous, ACS Reagent, ≥99.0%), 2-amino-3-hydroxypyridine ($C_5H_6N_2O$ and 98%) were bought from Sigma-Aldrich. $Cr(NO_3)_3{\cdot}9H_2O$) (99%) and hydrochloric acid (37%) were supplied by Merck KGaA (Darmstadt, Germany). All chemicals were of analytical grade.

pH studies were done with an Orion Brand pH Meter. Atomic absorption spectrometry (FAAS) (Analytik Jena, ContrAA 300) was used to determine Cr(III) in adsorption studies. While performing the modified and immobilized processes of Sp microcapsules, the characterization of each step was done with FTR (KBr pellets, 21°C temperature, 39% moisture, 1 atm pressure) and scanning electron microscopy (SEM).

2.2. Activation of Sporopollenin microcapsules

The hydroxyl groups of Sp were activated by adding 5.0 g of Sp to 50 mL of acetone in a 100 mL measuring flask and stirring. Afterward, it was kept under reflux for 4 h by mixing [20]. Active Sp recovered after filtration with a Büchner funnel was dried overnight at 60°C.

2.3. Preparation of Sp-CPTS

100 mL of dry toluene, 5.0 g of activated Sp microcapsules and 3 mL of 3-(chloropropyl)-trimethoxysilane (CPTS) were added to a 250 mL volumetric flask [21]. The suspension was refluxed for 72 h in sustained stirring at 110°C. It was filtered through the Büchner funnel. The filtrate was washed with C_7H_8, C_2H_5OH and CH_3OH and dried at 70°C for one day.

2.4. Preparation of the Sp-CPTS-AHP microcapsule biosorbent

100 mL of dry C7H8 was added to 5.0 g Sp-CPTS and 0.1 g of 2-amino-3-hydroxypyridine (AHP), and the consequent mix was mixed at 65°C for 12 h under reflux [22]. The suspension solution cooled to room temperature was filtered and the filtrate (Sp-CPTS-AHP) was washed sequentially with methanol, ethanol and diethyl ether. It was dried in a vacuum-packed oven at 60°C for one day. The possible structure and preparation steps of the Sp-CPTS-AHP microcapsule biosorbent are shown in Fig. 1 [22,23].

2.5. Batch method

Adsorption works were created to find the removal efficiency of Cr(III) with Sp-CPTS-AHP microcapsule

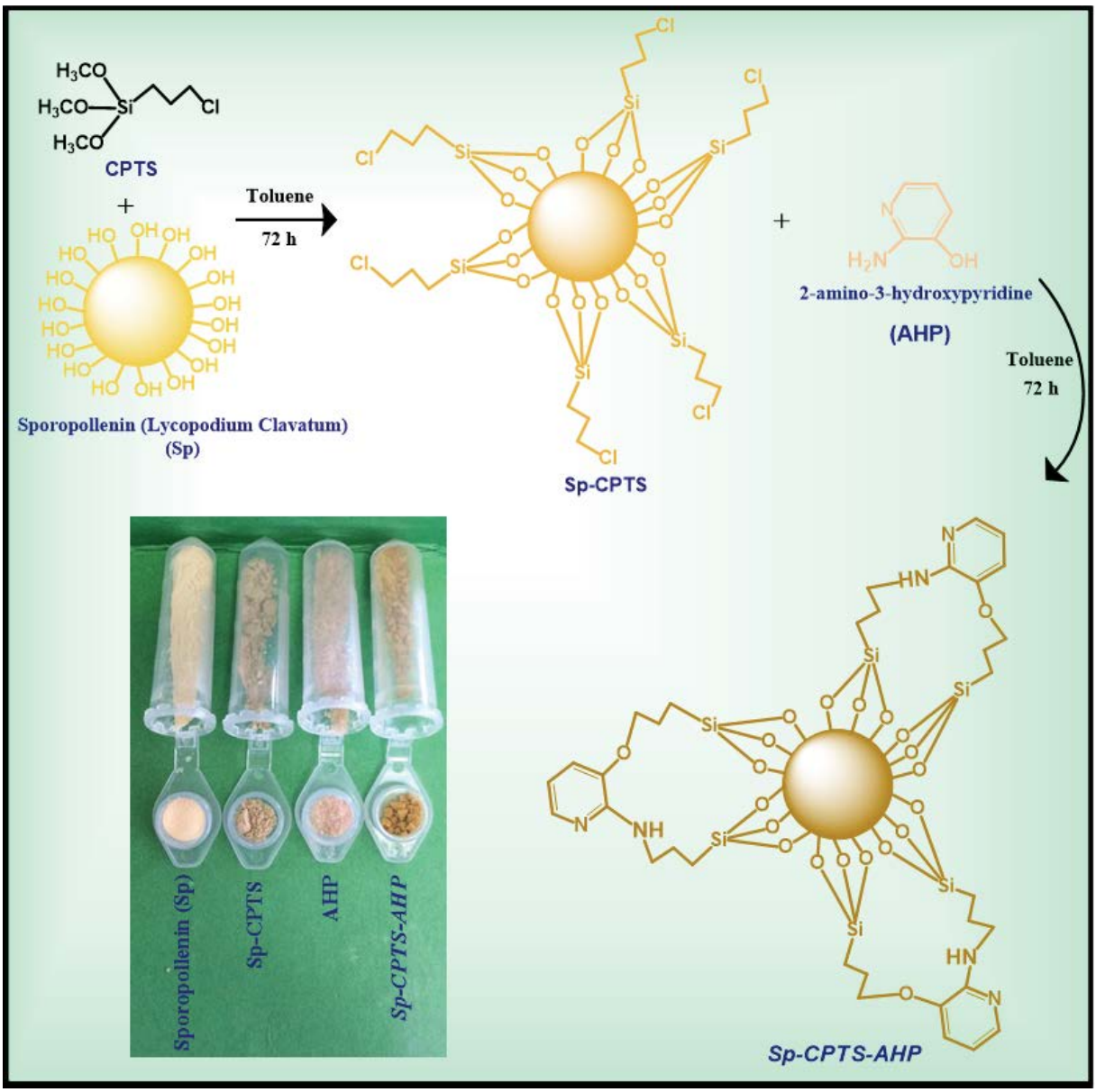

Fig. 1. The possible constructions of Sp, Sp-CPTS and Sp-CPTS-AHP.

biosorbent. The batch method was used in these experiments. Firstly, a 1000 mL solution containing Cr(III) ion (100 mg L^{-1}) was prepared from $Cr(NO_3)_3 \cdot 9H_2O$ with deionized water. The pH of the solutions containing Cr(III) was changed by the addition of 0.01 M HCl. Sp-CPTS-AHP microcapsule biosorbent (0.01–0.05 g), different temperatures (298.15–328.15 K), different pH (pH1.0–8.0), and different concentrations of Cr(III) ion solution (10–40 mg L^{-1})) was added to a 20 mL centrifuge tube containing. The suspension was filtered by shaking for an unlike duration (5–210 min). Cr(III) in the filtrate was measured by the FAAS method [24]. Using the calculated values and Eqs. (1)–(3), the adsorption equilibrium capacity q_e (mg g^{-1}) [25,26], the adsorption capacity q_t (mg g^{-1}) at a given time [27] and the percentage of removal (% removal) found [22].

$$q_e = \frac{C_o - C_e}{m} \times V \tag{1}$$

$$q_t = \frac{C_o - C_t}{m} \times V \tag{2}$$

$$\%\text{Removal} = \frac{C_o - C_e}{C_o} \times 100 \tag{3}$$

where V (L), m (g), C_e (mg L^{-1}), C_t (mg L^{-1}) and C_o (mg L^{-1}), Cr(III) represent the volume of the solution, the heft of Sp-CPTS-AHP, the concentration of Cr(III) after or in equilibrium, the Cr(III) concentration remaining in the

solution at any duration and the initial concentration of Cr(III) respectively [21].

3. Results and discussion

3.1. Characterization

3.1.1. SEM analysis

Surface morphologies of the Sp-CPTS-AHP microcapsule biosorbent were examined under SEM. SEM displays of Sp, Sp-CPTS and Sp-CPTS-AHP are demonstrated in Fig. 2. The SEM displays of the Sp (Fig. 2a) demonstrate a more straight morphology than the SEM displays of the Sp-CPTS (Fig. 2b) constituted after the modification of the CPTS to the surface. The pore form and geometrical construction of the Sp-CPTS-AHP microcapsule biosorbent disrupted are seen in Fig. 2c. It is seen as disordered morphology coated with alien substance, that is, AHP. The existence of connected particles, that is, AHP on the Sporopollenin surface verifies the immobilization [28].

3.1.2. Fourier-transform infrared spectroscopy analysis

The Fourier-transform infrared spectroscopy (FTIR) peaks of Sp, Sp-CPTS and Sp-CPTS-AHP are given in Fig. 3. In the FTIR peak of Sp, the peak originating from the –OH is 3,321 cm^{-1} [25]. Stretching vibration frequency originating from the aliphatic (–CH, $–CH_2$, $–CH_3$) group is between 2,850–2,921 cm^{-1}. Characteristic bands in the form of a double band belonging to the C=O group were seen at 1,706 cm^{-1} [7].

The peak of the –OH in Sp changed from 3,321 to 3,361 cm^{-1} in Sp-CPTS. Also, big peaks seen at 1,100 cm^{-1} represent C–O–C and Si–O–C or C–O and Si–O symmetrical or asymmetric stress [28].

It was determined that the peaks observed at 2,921–2,850 cm^{-1} belong to the CH stretching vibration frequencies in Sp-CPTS. In the Sp-CPTS spectrum, it was determined that there is an absorption band at 692 cm^{-1} in the silylating agent (CPTS) resulting from the C–Cl stretching vibration [29].

The peak of the –OH in Sp-CPTS changed from 3,361 to 3,354 cm^{-1} in the Sp-CPTS-AHP. The –C–N peak in Sp-CPTS-AHP was observed at 1,271 cm^{-1}. –C=N peak in Sp changed from 1,706 to 1,603 cm^{-1} in Sp-CPTS. The peaks observed in the range of 2,921–2,840 cm^{-1} in AHP and Sp-CPTS seem like three separate peaks in Sp-CPTS-AHP. This point out the existence of different CH, CH_2 or CH_3 in the constructions, which verifies that the AHP is immobilized to the Sp-CPTS.

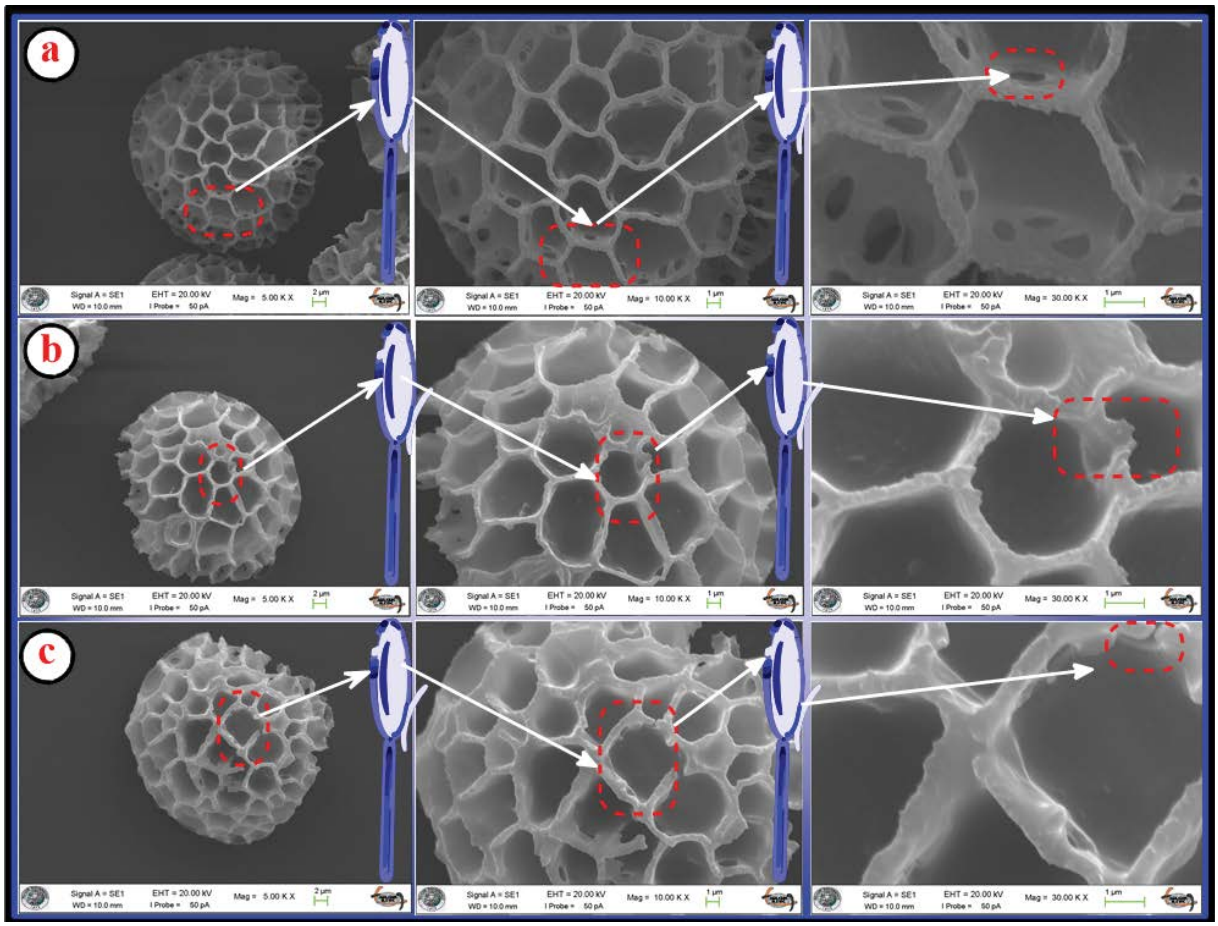

Fig. 2. SEM displays of the Lycopodium Clavatum Sporopollenin (a), (Sp-CPTS) (b) and the Sp-CPTS-AHP (c).

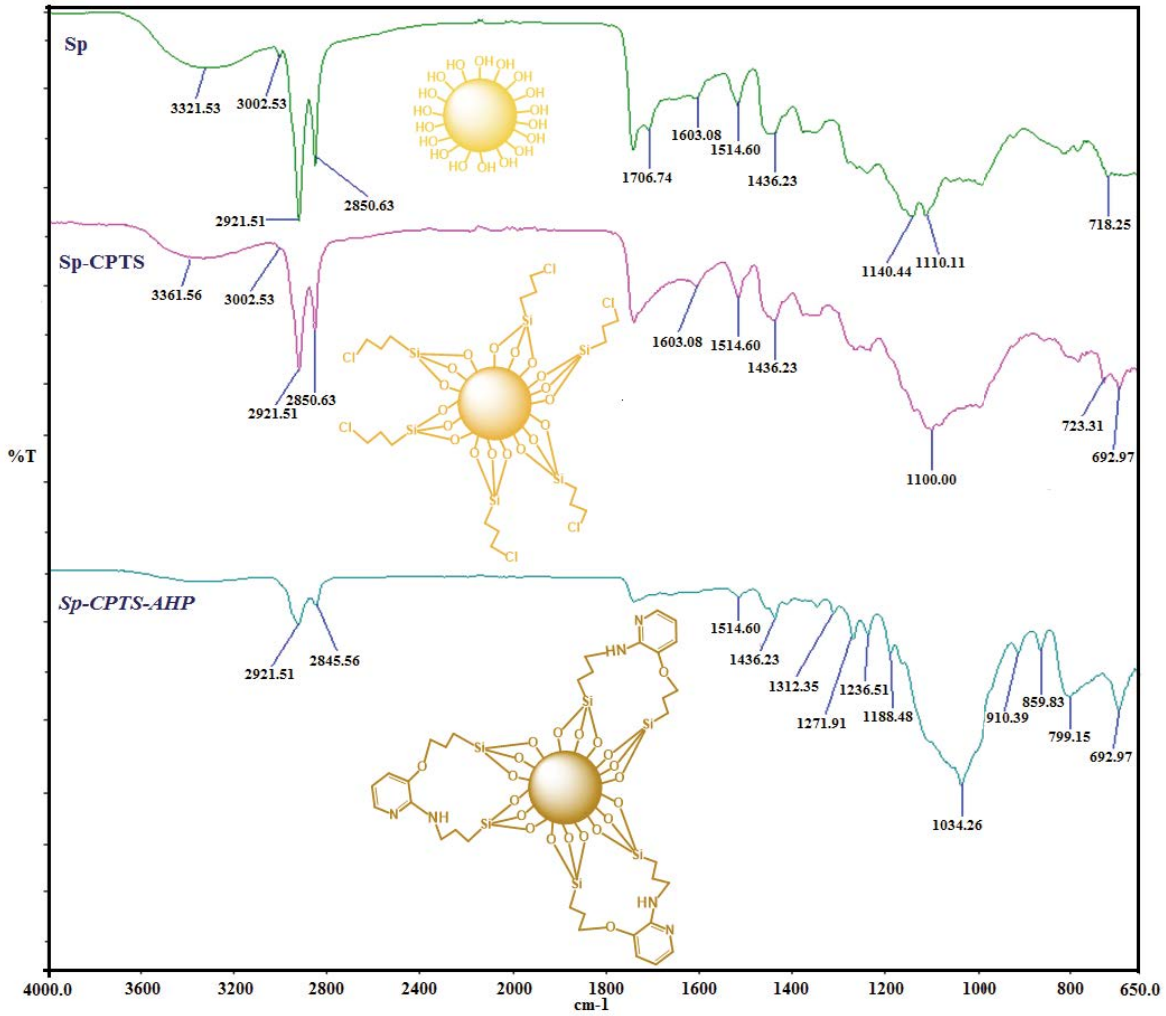

Fig. 3. FTIR spectra of the Sp (a), Sp-CPTS (b), and the Sp-CPTS-AHP (c).

3.2. Parameters affecting adsorption

3.2.1. pH

pH is one of the very significant factors impressing adsorption. Additionally, It determines the creation and steadiness of Cr(III). The adsorption performance could be impressed by diverse charge densities and Cr(III) on the Sp-CPTS-AHP microcapsule biosorbent surface. For this reason, some experiments were carried out to find the efficiency of the Sp-CPTS-AHP microcapsule biosorbent to adsorb Cr(III) ions in different pH ranges (1–8). The batch method was used in the experiments. According to the consequences found from the experimental works, the pH impress on the adsorption can be seen in Fig. 4a.

The pH of the chromium solution affects its adsorption on the Sp-CPTS-AHP microcapsule biosorbent, and the adsorption decreases with increasing pH. The presence of OH– ions in the environment causes chromium to form hydroxy complexes at higher pH values, $Cr(OH)_3$ [30].

Besides, Cr(III) removal decreased from 70% at pH 6 to 55% at pH 8 (Fig. 4a). Increasing the pH decreases the positive charges on the adsorbent surface. So, electrostatic pull happens among the (–) charges (NH_2^-, OH–) of the adsorbent and the (+) charges of the metal ions (Cr(III)), and the adsorption yield rises [31].

3.2.2. Contact time

Fig. 4b demonstrates the impact of contact time on the removal of Cr(III) ions. The percentages of removal of Cr(III) ions by the Sp-CPTS-AHP microcapsule biosorbent increased within the first 90 min (Fig. 4b) and removal efficiency of over 68% was obtained for the Cr(III) solution. Then, the removal efficiency of Cr(III) in the solution increased with time and; slowed down after reaching saturation. Adsorption has remained stable after 120 min.

3.2.3. Amount of adsorbent

The amount of Cr(III) adsorbed by Sp-CPTS-AHP microcapsule biosorbent was calculated by Eq. (2) and shown in Fig. 4c. As seen in Fig. 4c, Cr(III) removal increased as the

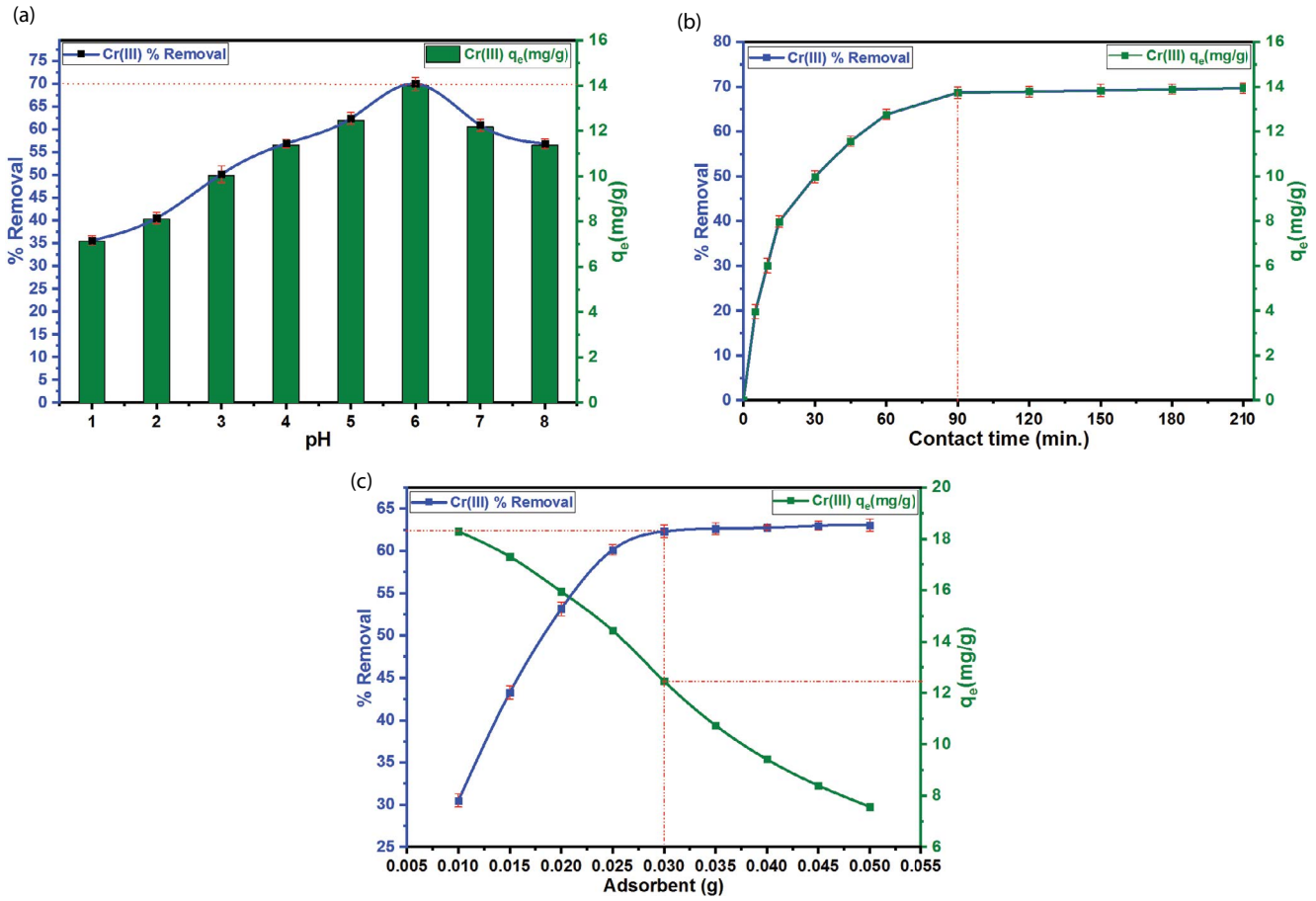

Fig. 4. (a) The impact of pH on the adsorption of Cr(III). (b) Influence of contact time on Cr(III) adsorption by the Sp-CPTS-AHP. (c) Effect of adsorbent amount on Cr(III) adsorption by the Sp-CPTS-AHP.

amount of adsorbent increased. The highest removal (63%) of Cr(III) in solution ($Cr(NO_3)_3{\cdot}9H_2O$) was achieved with 0.03 g adsorbent. According to this result, it can be said that the increase in Cr(III) removal is due to the expansion of the active surface area of the adsorbent. The adsorption capacity was lesser at higher adsorbent doses (Fig. 4c). This may be attributed to overlapping or aggregation of adsorption sites resulting in a decrease in total adsorbent surface area available to metal ions and an increase in diffusion path length [32].

3.2.4. Initial concentration and temperature

Fig. 6a shows how Cr(III) initial concentration affects adsorption. As can be seen from the graph, the adsorption capacity increased with the increase of Cr(III) amount and temperature. The percent removal in the initial concentration decreases with increasing temperature and concentration. After a certain time, the system attains balance and the surface field is filled. Thus, the adsorption process ends. In this study, the system reached equilibrium after 40 mg L^{-1}. Temperature also changes the thermodynamic parameters. The increased adsorption with temperature indicates that the adsorption reaction is endothermic.

3.3. Kinetics of adsorption

Kinetic data are needed to define the mechanism, occurrence, rate and efficiency of adsorption. Since the kinetics of the system checks the stay time of the adsorbed material and the size of the system, it is necessary to know the speed of adsorption when removing pollutants from water or wastewater [33]. In order to reach inter phase equilibrium and to sense how fast the metal ions move to the adsorbent, the removal time must be known. The experimental and theoretical data obtained were applied to the Equations in Table 1 and the pseudo-first-order and pseudo-second-order models to acquire kinetic datum (Fig. 5a and b) [34,35].

As seen in Table 1, the coefficient of correlation calculated with the pseudo-second-order model (q_e = 14.993 mg g^{-1}) is considerably higher than the coefficient of correlation calculated from the pseudo-first-order model (q_e = 7.568 mg g^{-1}). Considering these data, it seems more appropriate to explain the sorption kinetics with a pseudo-second-order model. In this case, it can be said that the adsorption takes place through electron sharing or electron exchange between the adsorbent and Cr(III).

Table 1
Kinetic adsorption parameters acquired using pseudo-first-order and pseudo-second-order models on Sp-CPTS-AHP

Kinetic models	Equations	References	Parameter constants	Parameter values	q_e(exp) (mg g^{-1})
Pseudo-first-order	$\log(q_e - q_t) = \log q_e - \frac{tk_1}{2.303}$	[36,37]	k_1 (min^{-1})	0.003	13.971
			q_e(calc) (mg g^{-1})	7.568	
			R_1^2	0.9414	
Pseudo-second-order	$\frac{t}{q_t} = \frac{1}{k_2 q_e^2} + \frac{t}{q_e}$	[38,39]	k_2 (g/(mg min)	0.0052	
			q_e(calc) (mg g^{-1})	14.993	
			R_2^2	0.999	

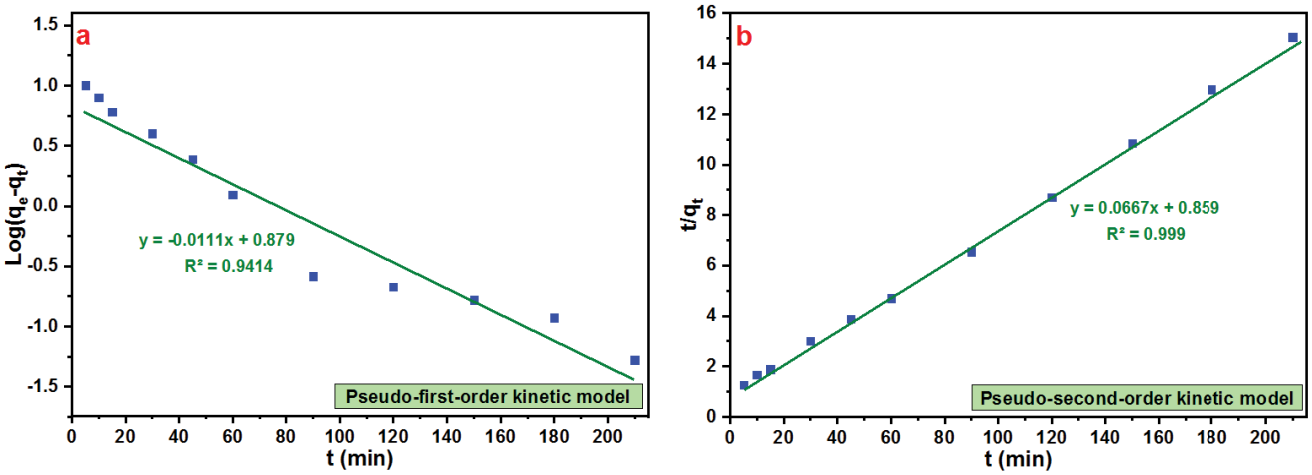

Fig. 5. Kinetic plots of (a) pseudo-first-order and (b) pseudo-second-order models for adsorption of Cr(III) on to Sp-CPTS-AHP.

3.4. Isotherms of adsorption

There are many isotherm models that explain the adsorption phenomenon [40]. In this work, the so-called Freundlich, Langmuir and Dubinin–Radushkevich isotherm models were used to elucidate the Cr(III) sorption on Sp-CPTS-AHP (Fig. 6b–d). Fig. 6a demonstrates the influence of the concentration of the starting solution on the adsorption of Cr(III) on the Sp-CPTS-AHP adsorbent. Adsorption studies were carried out under experimental conditions where chromium concentrations were between 10 and 50 mg L^{-1}, the contact time was 210 min, and pH was 6.0. As seen in Fig. 6a, as the chromium(III) concentration rises from 10 to 50 mg L^{-1}, the sorption capability increases and the elimination rate decreases from 97% to 55%. The decrease in % removal with the increase of chromium(III) ions is owing to the decrease of active fields on the adsorbent surface.

In addition, the increase in adsorption rate and ion utilization in active sites may clarify the rise in sorption capability [41]. Initial chromium(III) concentration is 30 mg L^{-1} for the most efficient elimination % and adsorption capacity.

Experimental data obtained to perform Cr(III) adsorption from an aqueous solution with Sp-CPTS-AHP at different temperatures were applied to the equations in Table 2. The obtained isotherm parameters are shown in the same table.

According to experimental data, the average energy of Cr(III) in solution is 0.893, 1.271, 1.549 and 2.744 kJ mol^{-1} for 298, 308, 318 and 328 K temperatures, respectively (Table 2). The average energy less of than 8 kJ mol^{-1} point out that the Cr(III) in the aqueous solution is physically adsorbed on the adsorbent [38]. Since the Langmuir isotherm with the highest R^2 value among the calculated isotherm parameters, the adsorption phenomenon can be explained by this isotherm (Table 2). In the Langmuir isotherm, adsorption occurs in a layer, and the maximum adsorption is when the molecules attached to the adsorbent surface create a satiated layer. Therefore, it can be thought that the Cr(III) adsorption in this study occurred in a monolayer.

3.5. Thermodynamic studies

It is important to know the thermodynamic features such as enthalpy change ($\Delta H°$), entropy change ($\Delta S°$) and free energy change ($\Delta G°$) to explain the sorption event and determine whether the process is spontaneous or not spontaneous [39]. In order to perform the adsorption of Cr(III) on the Sp-CPTS-AHP adsorbent, the efficacy of temperatures between 20°C and 50°C was researched. Thermodynamic feature for the adsorption of Cr(III) by Sp-CPTS-AHP are demonstrated in Table 3. Thermodynamic features were calculated from the equations in Table 3 and the outcomes found are demonstrated in the same table. In Table 3, positive $\Delta H°$

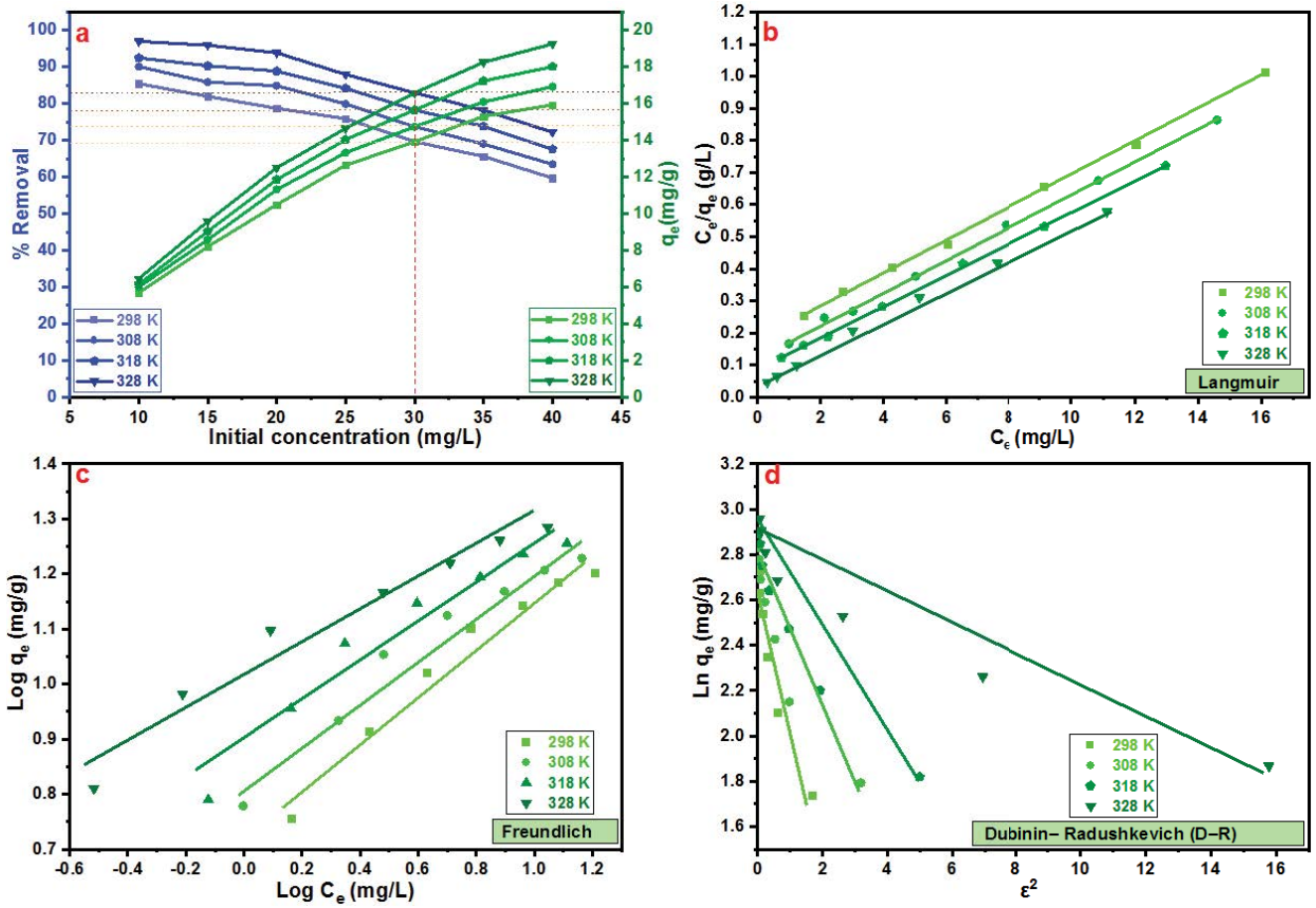

Fig. 6. Effect of initial Cr(III) concentration (a), Langmuir model (b) Freundlich model (c), and Dubinin–Radushkevich model of Cr(III) removal at different temperature (d).

Table 2
Adsorption isotherm model parameters for Cr(III) adsorption by Sp-CPTS-AHP at unlike temperatures

Model	Equation	References	Parameters	Temperature (K)			
				298	308	318	328
Langmuir	$\frac{C_e}{q_e}=\frac{C_e}{q_m}+\frac{1}{K_L q_m}$	[42–45]	R^2	0.9992	0.9986	0.9992	0.9982
			K_L (L mg^{-1})	0.3189	0.4115	0.5391	0.9764
			q_m (mg g^{-1})	17.668	19.646	20.704	21.929
	$R_L=\frac{1}{\left[1+\left(K_L.C_o\right)\right]}$		R_L	0.239–0.148	0.196–0.057	0.156–0.044	0.093–0.025
Freundlich	$\log q_e=\log K_F+\frac{1}{n}\log C_e$	[46,47]	R^2	0.9430	0.9560	0.9468	0.9748
			K_F (mg/g)·(mg/L)$^{-n}$	2.074	2.266	2.424	2.748
			$1/n$	0.3885	0.3844	0.376	0.3321
			n	2.574	2.601	2.660	3.011
Dubinin–Radushkevich	$\ln q_e \ln q_S-\beta\varepsilon^2$	[48–51]	R^2	0.9375	0.8727	0.8978	0.8443
			q_e (mg g^{-1})	13.629	14.732	15.892	16.728
	$\varepsilon=RT\ln\left[1+\frac{1}{C_e}\right]$		E (kJ mol^{-1})	0.893	1.271	1.549	2.744
	$E=\left(2\beta\right)^{-\frac{1}{2}}$						

Table 3
Thermodynamic feature and equations for the adsorption of Cr(III) by Sp-CPTS-AHP

Equation	References	Temperature (K)	$\Delta G°$ (kJ mol^{-1})	$\Delta S°$ (J mol^{-1} K^{-1})	$\Delta H°$ (kJ mol^{-1})
$\Delta G° = \Delta H° - T\Delta S°$	[52–54]	298	–41.02	235.88	29.31
$\Delta G° = -RT\ln K_e^o$		308	–43.38		
$nK_e^o = \frac{\Delta S°}{R} - \frac{\Delta H°}{RT}$		318	–45.73		
		328	–48.09		

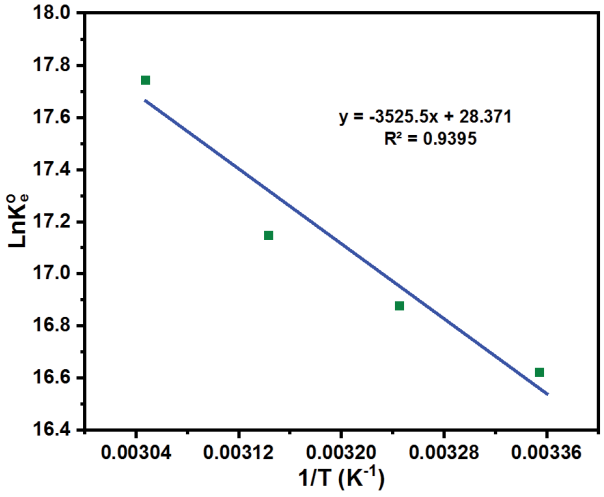

Fig. 7. Thermodynamic graph for the sorption of Cr(III) on Sp-CPTS-AHP.

and negative $\Delta G°$ indicate that the adsorption is endothermic and the adsorption reaction is spontaneous. The reduction in $\Delta G°$ value with increasing temperature point out that adsorption creation is inversely proportional to temperature. In addition, the positive $\Delta H°$ value supports this statement. A positive $\Delta S°$ value indicates the increase in random adsorption at the solid-solution interface and the happening of ion change reactions. Aqueous Cr(III) ions and water molecules form covalent bonds and bind to the adsorbent. For the water molecules are free, the rate of randomness, the kind of linking mechanism, and the adsorption energy of the respective binding increase the greatness of $\Delta H°$. Because of the little energy needed in physical adsorption, the adsorption operation is quick and usually reversible. The energy necessary for hydrogen bond creation and for London and van der Waals interactions is 4–8 and 8–40 kJ mol^{-1}, respectively. The $\Delta H°$ value for Cr(III) was obtained to be 29.31 kJ mol^{-1}.

The thermodynamic graph for the sorption of Cr(III) on Sp-CPTS-AHP is demonstrated in Fig. 7.

3.6. Comparison studies

The adsorbing capacity of the newly prepared Sp-CPTS-AHP microcapsule biosorbent was compared with the Sporopollenin supported and other adsorbent s shown in the sources and in Table 4. Considering these comparisons, it can be said that the adsorbing capacity of the Sp-CPTS-AHP microcapsule biosorbent is much better than other adsorbent materials.

3.7. Mechanism

The pH of the ambiance affects the creation of new and unlike types of Cr and the decomposition of active groups such as –OH, –COOH, –NH_2. That's why, Cr adsorption is highly correlated with pH. The existence of OH, C=O [8] and NH_2 in the Sp-CPTS-AHP microcapsule biosorbent was approved by FTIR [70]. The functional groups on the Sp-CPTS-AHP microcapsule biosorbent surface become positively charged at low pH and the approach of the cationic group is limited by the influence of repellent forces. With increasing pH, the degree of protonation reduces and functional groups are negatively charged (pH > pKa). Therefore, since there is no competing ion with Cr(III) ions, the highest adsorption takes place at pH = 6. The adsorption of Cr(III) can be clarified by an ion change mechanism.

According to the adsorption isotherms described above, the adsorption mechanism can be explained by the Langmuir isotherm model. According to this model, adsorption is chemical and adsorbs to the surface as a single layer [71]. It can be said that the adsorption of transmitter N_2 and OH groups on the surface with heavy metal ions occurs as a result of chemical adsorption [https://www.sciencedirect.com/science/journal/00219797/303/272]. The adsorption mechanism of Cr(III) in the Sp-CPTS-AHP microcapsule biosorbent is demonstrated in Fig. 8.

3.8. Recyclability of the Sp-CPTS-AHP

After desorption (Sp-CPTS-AHP) treatment, adsorption–desorption process was carried out to reuse Cr(III) ions. This process has been repeated many times. Sp-CPTS-AHP was incubated in 0.05 M EDTA for 120 min and the adsorbent was regenerated by treatment with Cr(III). Elimination efficiencies for Cr(III) are demonstrated in Fig. 9. The removal yield of Cr(III) with regenerated adsorbents appears to be greater than 62% even after four cycles (Fig. 9). For this reason, it can be recommended to reuse the prepared Sp-CPTS-AHP and it can be said that it has a high efficiency for Cr(III) removal.

4. Conclusion

The Sp-CPTS-AHP microcapsule biosorbent was originally prepared. The structure of this biosorbent was

Table 4
Comparison of the adsorbing capability of Sp-CPTS-AHP for Cr(III) in aqueous solution with other adsorbent materials

Adsorbent materials	Maximum adsorbing capacity (mg g^{-1})	References
Magnetite nanoparticle	1.1	[55]
Activated charcoal	0.9614	[56]
Coconut shell charcoal	3.65	[57]
Bagasse fly ash	4.35	[58]
Sunflower stem	6.2	[59]
CaO/Fe_3O_4/SDS nanocomposite	6.402	[60]
Coir pith	9.4	[61]
TiO_2 beads	10	[62]
Oats	12.9	[63]
JFP	13.5	[64]
Thermally modified fly ash	14.65	[65]
Zincon-modified activated carbon	17.9	[66]
Scrap iron	19	[67]
Organomodified diatomaceous earth	22.78	[68]
G3-PAMAM-SBA-15	23	[69]
298 K	17.668	This work
Sp-CPTS-AHP 308 K	21.929	
318 K	20.704	
328 K	21.929	

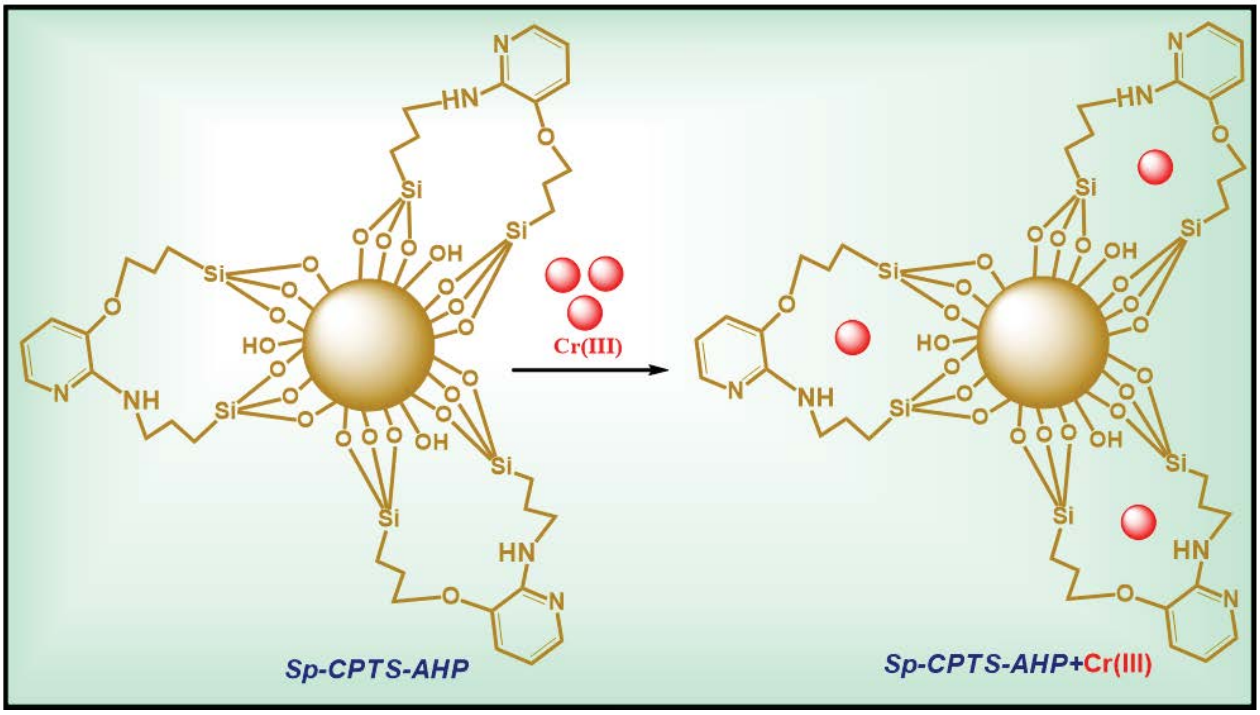

Fig. 8. Adsorption mechanism of Cr(III) on Sp-CPTS-AHP microcapsule biosorbent.

approved by FTIR and SEM. According to the experimental results with Sp-CPTS-AHP, it has been seen to have a good separation capacity (~70%). It is also insoluble in many acids and water and is economical, convenient for removal of heavy metals from wastewater, and has a wide active surface field. In addition, the Cr(III) removal efficiency of the regenerated adsorbent is more than 62% even after four cycles (Fig. 9). This result shows that the

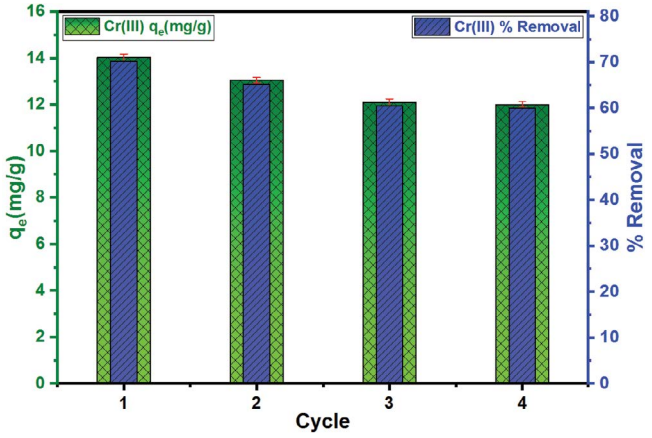

Fig. 9. Regeneration performance of Sp-CPTS-AHP microcapsule biosorbent (pH = 6.0, temperature = 298 K, adsorbent dose = 0.03 g, and initial concentration of Cr(III) = 30 mg L^{-1}).

prepared adsorbent can be used many times in chrome removal.

According to the parameters interpreted from the experimental data, the best Cr removal was attained at pH = 6.0, 0.03 g adsorbent, 298 K temperature, 30 mg L^{-1} initial concentration and 90 min contact time.

Among the calculated isotherm parameters, the Langmuir isotherm model has the highest R^2 (0.9992) value (Table 2). The adsorption fact can be clarified by the Langmuir isotherm model. Because the experimental parameters show that the adsorption fits this isotherm model. In accordance with this model, adsorption happens in a single layer. According to the correlation coefficients in Table 1, it is more appropriate to explain the adsorption kinetics with a pseudo-second-order model. In this case, it can be thought that the adsorption takes place through electron sharing or electron exchange between the adsorbent and Cr(III) [11]. Consequently, in experimental studies, the average energy of Cr(III) in solution is 0.893, 1.271, 1.549 and 2.744 kJ mol^{-1} for 298, 308, 318 and 328 K temperatures, respectively. According to this result, it can be said that the reaction on the adsorbent occurs physically. The average free energy (E) obtained for Cr(III) ions based on the Dubinin–Radushkevich isotherm is less than 8 kJ mol^{-1}. This result indicates that physical adsorption is involved to the chemically occurring adsorption process [73].

The $\Delta H°$ value for Cr(III) was obtained to be 29.31 kJ mol^{-1}. Also, the $\Delta G°$ values are –41.02, –43.38, –45.73, –48.09 kJ mol^{-1} for 298°C, 308°C, 318°C and 328°C, respectively. The positive $\Delta H°$ value of the calculated thermodynamic parameters shows that the adsorption reaction is endothermic and the negative $\Delta G°$ value indicates that the reaction is spontaneous. This work is suitable for the removal of Cr(III) and toxic metals from wastewater, it is a newly developed microcapsule adsorbent, it is economical and it can be used many times. It may also offer new opportunities to develop a suitable and economical process for the removal of Cr(III) and toxic metals from wastewater [74,75].

Acknowledgments

The author sincerely thanks the management of Karamanoglu Mehmetbey University Kamil Ozdag Faculty of Science and Department of Chemistry for providing the necessary opportunities for this study.

References

[1] M.L. Sall, A.K.D. Diaw, D. Gningue-Sall, S. Efremova Aaron, J.-J. Aaron, Toxic heavy metals: impact on the environment and human health, and treatment with conducting organic polymers, a review, Environ. Sci. Pollut. Res., 27 (2020) 29927–29942.
[2] T.O. Ajiboye, O.A. Oyewo, D.C. Onwudiwe, Simultaneous removal of organics and heavy metals from industrial wastewater: a review, Chemosphere, 26 (2021) 128379, doi: 10.1016/j.chemosphere.2020.128379.
[3] S. Ali, Z. Abbas, M. Rizwan, I.E. Zaheer, I. Yavaş, A. Ünay, M.M. Abdel-DAIM, M. Bin-Jumah, M. Hasanuzzaman, D. Kalderis, Application of floating aquatic plants in phytoremediation of heavy metals polluted water: a review, Sustainability, 12 (2020) 1927, doi: 10.3390/su12051927.
[4] C. Santhosh, R. Nivetha, P. Kollu, V. Srivastava, M. Sillanpää, A.N. Grace, A. Bhatnagar, Removal of cationic and anionic heavy metals from water by 1D and 2D-carbon structures decorated with magnetic nanoparticles, Sci. Rep., 7 (2017) 14107, doi: 10.1038/s41598-017-14461-2.
[5] A. Singh, P. Khare, S. Verma, A. Bhati, A.K. Sonker, K.M. Tripathi, S.K. Sonkar, Pollutant soot for pollutant dye degradation: soluble graphene nanosheets for visible light induced photodegradation of methylene blue, ACS Sustainable Chem. Eng., 5 (2017) 8860–8869.
[6] T.S. Anirudhan, S.S. Sreekumari, Adsorptive removal of heavy metal ions from industrial effluents using activated carbon derived from waste coconut buttons, J. Environ. Sci., 23 (2011) 1989–1998.
[7] A.H. Mahvi, D. Balarak, E. Bazrafshan, Remarkable reusability of magnetic Fe_3O_4-graphene oxide composite: a highly effective adsorbent for Cr(VI) ions, Int. J. Environ. Anal. Chem., (2021) 1–21, doi: 10.1080/03067319.20211910250.
[8] X. Fang, J. Li, X. Li, S. Pan, X. Zhang, X. Sun, J. Shen, W. Han, L. Wang, Internal pore decoration with polydopamine nanoparticle on polymeric ultrafiltration membrane for enhanced heavy metal removal, Chem. Eng. J., 314 (2017) 38–49.
[9] Y. Li, Z. Xu, S. Liu, J. Zhang, X. Yang, Molecular simulation of reverse osmosis for heavy metal ions using functionalized nanoporous graphenes, Comput. Mater. Sci., 139 (2017) 65–74.
[10] B. Eyvazi, A. Jamshidi-Zanjani, A.K. Darban, Immobilization of hexavalent chromium in contaminated soil using nano-magnetic $MnFe_2O_4$, J. Hazard. Mater., 365 (2019) 813–819.
[11] Y. Qiu, Q. Zhang, B. Gao, M. Li, Z. Fan, W. Sang, H. Hao, X. Wei, Removal mechanisms of Cr(VI) and Cr(III) by biochar supported nanosized zero-valent iron: synergy of adsorption, reduction and transformation, Environ. Pollut., 265 (2020) 115018, doi: 10.1016/j.envpol.2020.115018.
[12] S. Martini, S. Afroze, K.A. Roni, Modified eucalyptus bark as a sorbent for simultaneous removal of COD, oil, and Cr(III) from industrial wastewater, Alexandria Eng. J., 59 (2020) 1637–1648.
[13] L. Vimercati, M.F. Gatti, T. Gagliardi, F. Cuccaro, L. De Maria, A. Caputi, M. Quarato, A. Baldassarre, Environmental exposure to arsenic and chromium in an industrial area, Environ. Sci. Pollut. Res., 24 (2017) 11528–11535.
[14] Y. Ye, X. Yu, L. Zhang, Q. Li, F. Pan, D. Xia, Effect of organic ligands on the removal of Cr(III) from water by coagulation process, Desal. Water Treat., 228 (202) 253–260.
[15] J. Zhang, C.H. Xue, H.R. Ma, Y.R. Ding, S.T. Jia, Fabrication of PAN electrospun nanofibers modified by tannin for effective

removal of trace Cr(III) in organic complex from wastewater, Polymers, 12 (2020) 210, doi: 10.3390/polym12010210.
[16] P.B. Tchounwou, C.G. Yedjou, A.K. Patlolla, D.J. Sutton, Heavy metals toxicity and the environment, Mol. Clin. Environ. Toxicol., 101 (2012) 133–164.
[17] D. Huang, G. Wang, Z. Shi, Z. Li, F. Kang, F. Liu, Removal of hexavalent chromium in natural groundwater using activated carbon and cast iron combined system, J. Cleaner Prod., 165 (2017) 667–676.
[18] K.G. Pavithra, P.S. Kumar, F.C. Christopher, A. Saravanan, Removal of toxic Cr(VI) ions from tannery industrial wastewater using a newly designed three-phase three-dimensional electrode reactor, J. Phys. Chem. Solids, 110 (2017) 379–385.
[19] G. Wang, Q. Chang, M. Zhang, X. Han, Effect of pH on the removal of Cr(III) and Cr(VI) from aqueous solution by modified polyethyleneimine, React. Funct. Polym., 73 (2013) 1439–1446.
[20] L. Pietrelli, I. Francolini, A. Piozzi, M. Sighicelli, I. Silvestro, M. Vocciante, Chromium(III) removal from wastewater by chitosan flakes, Appl. Sci., 10 (2020) 1925, doi: 10.3390/app10061925.
[21] A. Çimen, M. Torun, A. Bilgiç, Immobilization of 4-amino-2-hydroxyacetophenone onto silica gel surface and sorption studies of Cu(II), Ni(II), and Co(II) ions, Desal. Water Treat., 53 (2015) 2106–2116.
[22] Y. Du, M. Dai, J. Cao, C. Peng, Fabrication of a low-cost adsorbent supported zero-valent iron by using red mud for removing Pb(II) and Cr(VI) from aqueous solutions, RSC Adv., 9 (2019) 33486–33496.
[23] A. Çimen, A. Bilgiç, İ. Yılmaz, Chemical modification of silica gel with hydrazine carbothioamide derivative for sorption studies of Cu(II), Ni(II) and Co(II) ions, Desal. Water Treat., 55 (2015) 420–430.
[24] Y. Tang, J. Zhao, J. Zhao, Y. Zeng, W. Zhang, B. Shi, Highly efficient removal of Cr(III)-poly(acrylic acid) complex by co-precipitation with polyvalent metal ions: performance, mechanism, and validation, Water Res., 178 (2020) 115807, doi: 10.1016/j.watres.2020.115807.
[25] A. Çimen, A. Bilgiç, Removal of Cu(II), Co(II) and Ni(II) ions from aqueous solutions using modified Sporopollenin, J. Appl. Biol. Sci., 12 (2018) 42–44.
[26] T. Guimarães, L.D. Paquini, B.R.L. Ferraz, L.P.R. Profeti, D. Profeti, Efficient removal of Cu(II) and Cr(III) contaminants from aqueous solutions using marble waste powder, J. Environ. Chem. Eng., 8 (2020) 103972, doi: 10.1016/j.jece.2020.103972.
[27] G.P. Schoeler, T.F. Afonso, R. de Avila Delucis, B.C. Okeke, R. Andreazza, Removal of Cr(III) from water by polyurethane foam incorporated with green liquor dregs waste, Europe BMC, (2021), doi: 10.21203/rs.3.rs-595298/v1.
[28] A. Bilgiç, H.S. Karapınar, APTMS-BCAD modified magnetic iron oxide for magnetic solid-phase extraction of Cu(II) from aqueous solutions, Heliyon, 8 (2022) e09645, doi: 10.1016/j.heliyon.2022.e09645.
[29] J. Liu, Y. Chen, S. Jiang, J. Huang, Y. Lv, Y. Liu, M. Liu, Rapid removal of Cr(III) from high-salinity wastewater by cellulose-g-poly-(acrylamide-co-sulfonic acid) polymeric bio-adsorbent, Carbohydr. Polym., 270 (2021) 118356, doi: 10.1016/j.carbpol.2021.118356.
[30] M. Naushad, T. Ahamad, G. Sharma, H. Ala'a, A.B. Albadarin, M.M. Alam, A.A. Ghfar, Synthesis and characterization of a new starch/SnO_2 nanocomposite for efficient adsorption of toxic Hg^{2+} metal ion, Chem. Eng. J., 300 (2016) 306–316.
[31] S. Zhang, C. Liu, Y. Yuan, M. Fan, D. Zhang, D. Wang, Y. Xu, Selective, highly efficient extraction of Cr(III), Pb(II) and Fe(III) from complex water environment with a tea residue derived porous gel adsorbent, Bioresour. Technol., 311 (2020) 123520, doi: 10.1016/j.biortech.2020.123520.
[32] J. Wang, Y. Chen, T. Sun, A. Saleem, C. Wang, Enhanced removal of Cr(III)-EDTA chelates from high-salinity water by ternary complex formation on DETA functionalized magnetic carbon-based adsorbents, Ecotoxicol. Environ. Saf., 209 (2021) 111858, doi: 10.1016/j.ecoenv.2020.111858.
[33] D. Balarak, H. Azarpira, F.K. Mostafapour, Thermodynamics of removal of cadmium by adsorption on Barley husk biomass, Der Pharma Chemica, 8 (2016) 243–247.
[34] A. Cimen, A. Bilgic, Immobilization of 2-(2-hydroxybenzylidinoamino) pyridin-3-ol on silica gel and application to industrial wastewater, Desal. Water Treat., 147 (2019) 116–124.
[35] C. Bai, L. Wang, Z. Zhu, Adsorption of Cr(III) and Pb(II) by graphene oxide/alginate hydrogel membrane: characterization, adsorption kinetics, isotherm and thermodynamics studies, Int. J. Biol. Macromol., 147 (2020) 898–910.
[36] H. Wu, Y. Xiao, Y. Guo, S. Miao, Q. Chen, Z. Chen, Functionalization of SBA-15 mesoporous materials with 2-acetylthiophene for adsorption of Cr(III) ions, Microporous Mesoporous Mater., 292 (2020) 109754, doi: 10.1016/j.micromeso.2019.109754.
[37] L. Wu, W. Wan, Z. Shang, X. Gao, N. Kobayashi, G. Luo, Z. Li, Surface modification of phosphoric acid activated carbon by using non-thermal plasma for enhancement of Cu(II) adsorption from aqueous solutions, Sep. Purif. Technol., 197 (2018) 156–169.
[38] Y. Ho, J. Ng, G. McKay, Kinetics of pollutant sorption by biosorbents, Sep. Purif. Methods, 29 (2000) 189–232.
[39] S. Anush, B. Vishalakshi, Modified chitosan gel incorporated with magnetic nanoparticle for removal of Cu(II) and Cr(VI) from aqueous solution, Int. J. Biol. Macromol., 133 (2019) 1051–1062.
[40] Y. Ren, X. Wei, M. Zhang, Adsorption character for removal Cu(II) by magnetic Cu(II) ion imprinted composite adsorbent, J. Hazard. Mater., 158 (2008) 14–22.
[41] J. Wang, M. Mao, S. Atif, Y. Chen, Adsorption behavior and mechanism of aqueous Cr(III) and Cr(III)-EDTA chelates on DTPA-chitosan modified Fe_3O_4@SiO_2, React. Funct. Polym., 156 (2020) 104720, doi: 10.1016/j.reactfunctpolym.2020.104720.
[42] M. Cea, J. Seaman, A. Jara, M. Mora, M. Diez, Kinetic and thermodynamic study of chlorophenol sorption in an allophanic soil, Chemosphere, 78 (2010) 86–89.
[43] J. Zhang, M. Yan, G. Sun, K. Liu, An environment-friendly Fe_3O_4@CFAS porous ceramic: adsorption of Cu(II) ions and process optimisation using response surface methodology, Ceram. Int., 47 (2021) 8256–8264.
[44] I. Langmuir, The adsorption of gases on plane surfaces of glass, mica and platinum, J. Am. Chem. Soc., 40 (1918) 1361–1403.
[45] M. Mubarak, H. Jeon, M.S. Islam, C. Yoon, J.-S. Bae, S.-J. Hwang, W. San Choi, H.-J. Lee, One-pot synthesis of layered double hydroxide hollow nanospheres with ultrafast removal efficiency for heavy metal ions and organic contaminants, Chemosphere, 201 (2018) 676–686.
[46] A. Çimen, A. Bilgiç, İ. Yılmaz, A. Cukurovali, Chemical modification of silica gel surface with a carbothioamide Schiff base for removal of Cr(III) ions from wastewater samples, Desal. Water Treat., 183 (2020) 222–232.
[47] W. Liu, J. Ni, X. Yin, Synergy of photocatalysis and adsorption for simultaneous removal of Cr(VI) and Cr(III) with TiO_2 and titanate nanotubes, Water Res., 53 (2014) 12–25.
[48] N.C. Joshi, K. Kaur, N. Kumar, N.S. Bhandari, A. Thakur, Synthesis and adsorption applications of PPY/Fe_3O_4 nano-composite based material, Nano-Struct. Nano-Objects, 25 (2021) 100669, doi: 10.1016/j.nanoso.2021.100669.
[49] C.-J. Tang, X. Chen, F. Feng, Z.-G. Liu, Y.-X. Song, Y.-Y. Wang, X. Tang, Roles of bacterial cell and extracellular polymeric substance on adsorption of Cu(II) in activated sludges: a comparative study, J. Water Process Eng., 41 (2021) 102094, doi: 10.1016/j.jwpe.2021.102094.
[50] A. Gamal, A.G. Ibrahim, E.M. Eliwa, A.H. El-Zomrawy, S.M. El-Bahy, Synthesis and characterization of a novel benzothiazole functionalized chitosan and its use for effective adsorption of Cu(II), Int. J. Biol. Macromol., 183 (2021) 1283–1292.
[51] A. Bilgiç, A. Çimen, Synthesis, characterization, adsorption studies and comparison of superparamagnetic iron oxide nanoparticles (SPION) with three different amine groups functionalized with BODIPY for the removal of Cr(VI) metal

ions from aqueous solutions, Int. J. Environ. Anal. Chem., (2021) 1–26, doi: 10.1080/03067319.2021.1884240.
[52] A. Bilgiç, A. Çimen, Removal of chromium(VI) from polluted wastewater by chemical modification of silica gel with 4-acetyl-3-hydroxyaniline, RSC Adv., 9 (2019) 37403–37414.
[53] E.C. Lima, A. Hosseini-Bandegharaei, J.C. Moreno-Piraján, I. Anastopoulos, A critical review of the estimation of the thermodynamic parameters on adsorption equilibria. Wrong use of equilibrium constant in the Van't Hoof equation for calculation of thermodynamic parameters of adsorption, J. Mol. Liq., 273 (2019) 425–434.
[54] Y. Liu, Is the free energy change of adsorption correctly calculated?, J. Chem. Eng. Data, 54 (2009) 1981–1985.
[55] E.C. Lima, A.A. Gomes, H.N. Tran, Comparison of the nonlinear and linear forms of the van't Hoff equation for calculation of adsorption thermodynamic parameters ($\Delta S°$ and $\Delta H°$), J. Mol. Liq., 311 (2020) 113315, doi: 10.1016/j.molliq.2020.113315.
[56] M. Tahergorabi, A. Esrafili, M. Kermani, M. Shirzad-Siboni, Application of thiol-functionalized mesoporous silica-coated magnetite nanoparticles for the adsorption of heavy metals, Desal. Water Treat., 57 (2016) 19834–19845.
[57] S. Mor, K. Ravindra, N. Bishnoi, Adsorption of chromium from aqueous solution by activated alumina and activated charcoal, Bioresour. Technol., 98 (2007) 954–957.
[58] S. Babel, T.A. Kurniawan, Cr(VI) removal from synthetic wastewater using coconut shell charcoal and commercial activated carbon modified with oxidizing agents and/or chitosan, Chemosphere, 54 (2004) 951–967.
[59] V.K. Gupta, I. Ali, Removal of lead and chromium from wastewater using bagasse fly ash-a sugar industry waste, J. Colloid Interface Sci., 271 (2004) 321–328.
[60] U.R. Malik, S.M. Hasany, M.S. Subhani, Sorptive potential of sunflower stem for Cr(III) ions from aqueous solutions and its kinetic and thermodynamic profile, Talanta, 66 (2005) 166–173.
[61] S. Tamjidi, H. Esmaeili, Chemically modified CaO/Fe_3O_4 nanocomposite by sodium dodecyl sulfate for Cr(III) removal from water, Chem. Eng. Technol., 42 (2019) 607–616.
[62] M.F. Sawalha, J.R. Peralta-Videa, G.B. Saupe, K.M. Dokken, J.L. Gardea-Torresdey, Using FTIR to corroborate the identity of functional groups involved in the binding of Cd and Cr to saltbush (*Atriplex canescens*) biomass, Chemosphere, 66 (2007) 1424–1430.
[63] N. Wu, H. Wei, L. Zhang, Efficient removal of heavy metal ions with biopolymer template synthesized mesoporous titania beads of hundreds of micrometers size, Environ. Sci. Technol., 46 (2012) 419–425.
[64] G.-R.R. Bernardo, R.-M.J. Rene, Chromium(III) uptake by agro-waste biosorbents: chemical characterization, sorption–desorption studies, and mechanism, J. Hazard. Mater., 170 (2009) 845–854.
[65] S. Ranasinghe, A. Navaratne, N. Priyantha, Enhancement of adsorption characteristics of Cr(III) and Ni(II) by surface modification of jackfruit peel biosorbent, J. Environ. Chem. Eng., 6 (2018) 5670–5682.
[66] F. Han, L. Wang, Y. Li, S. Di, Application of thermally modified fly ash for adsorption of Ni(II) and Cr(III) from aqueous solution: equilibrium, kinetic, and thermodynamic studies, Environ. Eng. Sci., 34 (2017) 508–515.
[67] Z. Li, X. Chang, Z. Hu, X. Huang, X. Zou, Q. Wu, R. Nie, Zincon-modified activated carbon for solid-phase extraction and preconcentration of trace lead and chromium from environmental samples, J. Hazard. Mater., 166 (2009) 133–137.
[68] M. Gheju, A. Iovi, I. Balcu, Hexavalent chromium reduction with scrap iron in continuous-flow system: Part 1: Effect of feed solution pH, J. Hazard. Mater., 153 (2008) 655–662.
[69] R.A. Abu-Zurayk, R.Z. Al Bakain, I. Hamadneh, A.H. Al-Dujaili, Adsorption of Pb(II), Cr(III) and Cr(VI) from aqueous solution by surfactant-modified diatomaceous earth: equilibrium, kinetic and thermodynamic modeling studies, Int. J. Miner. Process, 140 (2015) 79–87.
[70] Y. Jiang, Q. Gao, H. Yu, Y. Chen, F. Deng, Intensively competitive adsorption for heavy metal ions by PAMAM-SBA-15 and EDTA-PAMAM-SBA-15 inorganic–organic hybrid materials, Microporous Mesoporous Mater., 103 (2007) 316–324.
[71] A. Çimen, A. Bilgiç, B. Karademir, Synthesis of eco-friendly Sp-EN-CPA adsorbent and its application for removal of Cr(VI) from aqueous solutions, Desal. Water Treat., 225 (2021) 287–299.
[72] D. Balarak, M. Zafariyan, C.A. Igwegbe, K.K. Onyechi, J.O. Ighalo, Adsorption of acid blue 92 dye from aqueous solutions by single-walled carbon nanotubes: isothermal, kinetic, and thermodynamic studies, Environ. Processes, 8 (2021) 869–888.
[73] X. Han, Y.S. Wong, N.F.Y. Tam, Surface complexation mechanism and modeling in Cr(III) biosorption by a microalgal isolate, *Chlorella miniata*, J. Colloid Interface Sci., 303 (2006) 365–371.
[74] W.W. Ngah, S. Fatinathan, Adsorption characterization of Pb(II) and Cu(II) ions onto chitosan-tripolyphosphate beads: kinetic, equilibrium and thermodynamic studies, J. Environ. Manage., 91 (2010) 958–969.
[75] F. Kiliçel, H. Karapinar, Determination of trace element contents of some spice samples by using FAAS, Asian J. Chem., 30 (2018) 1551–1558.